

17 **Abstract**

18 Roads can have a significant impact on the frequency of mass wasting events in mountainous
19 areas. However, characterizing the extent and pervasiveness of landslides over time rarely been
20 documented due to limitations in available data sources to consistently map such events. We
21 monitored the evolution of a road network and assessed its effect on slope stability for a ten year
22 window in Arhavi, Turkey. The main road construction projects run in the area are associated
23 with a hydroelectric power plant as well as other road extension works and are clearly associated
24 with the vast majority (90.1%) of mass movements in the area. We also notice that the overall
25 number and size of the landslides are much larger than in the naturally-occurring comparison
26 area. This marks a strong and negative effect of human activities on the natural course of earth
27 surface processes. Our findings show that the damage generated by the road construction is
28 compatible with the possible effect of a theoretical earthquake with a magnitude greater than
29 $M_w=6.0$. Overall, better co- and post-construction conditions should be ensured during and after
30 road works to mitigate the risk to local communities. We also notice a significant variation in
31 sediment transport as a result of road construction. As a result, our study fits in the big picture of
32 Anthropocene related changes and specifically points out at problems in mountainous areas that
33 could undoubtedly be better managed to reduce the risk to local communities.

34 **1 Introduction**

35 Recent findings suggest that our planet has been going through a new geologic time,
36 Anthropocene, in which human-driven changes dominate the Earth system and its geological
37 records instead of natural processes (e.g., Lewis & Maslin, 2015; Steffen, Broadgate, Deutsch,
38 Gaffney, & Ludwig, 2015). The existence of the Anthropocene is supported by the “*Great*
39 *Acceleration*” graphs showing proxies of growing human activities (e.g., population, water use,
40 transportation, etc.,) and their influence on natural systems (e.g., CO₂ emission, surface
41 temperature, domesticated land, etc.,), which becomes quite obvious since the mid-20th century
42 (Steffen et al., 2015; Steffen, Grinevald, Crutzen, & McNeill, 2011) and is functionally and
43 stratigraphically distinct from the Holocene epoch (Waters et al., 2016). However, the existence
44 of the Anthropocene still needs much evidence (Brown et al., 2013). Notably, soil erosion, as a
45 geomorphologic process, has an essential role in the formation of the geological record. In fact,
46 soil erosion in the Anthropocene is chiefly governed by the coupled effect of natural and human-

47 induced soil erosion processes (Poesen, 2018). In this context, we still need to better understand
 48 the interactions between these processes (Brown et al., 2017).

49 In seismically active mountain ranges, landslides appear as the major erosive agent (e.g., Dadson
 50 et al., 2004; Morin et al., 2018; Parker et al., 2011). Moreover, anthropogenic factors (i.e., land-
 51 use change, deforestation, hill cutting, etc.) can also be a significant contributor of landslide
 52 initiations in active mountain ranges (e.g., Chang & Slaymaker, 2002; Holcombe, Beesley,
 53 Vardanega, & Sorbie, 2016; Larsen & Parks, 1997; Vuillez et al., 2018). In particular, road
 54 construction is reported as one of the most influential factors of landslide occurrence in
 55 seismically active mountainous regions such as in India (e.g., Barnard, Owen, Sharma, & Finkel,
 56 2001; Haigh, Rawat, & Bartarya, 1989), Nepal (e.g., Hearn & Shakya, 2017; McAdoo et al.,
 57 2018), New Zealand (e.g., Coker & Fahey, 1993; Fransen, Phillips, & Fahey, 2001), Pakistan
 58 (e.g., Atta-ur-Rahman, Khan, Collins, & Qazi, 2011; Owen et al., 2008) and Taiwan (e.g., Chang
 59 & Slaymaker, 2002; Chen & Chang, 2011). This is not a surprising because hillslope cutting can
 60 cause a reduction in shear strength of hill slope material and also raised or perched water tables
 61 that lead to increase pore water pressure in case of rainfall event (Holcombe et al., 2016).

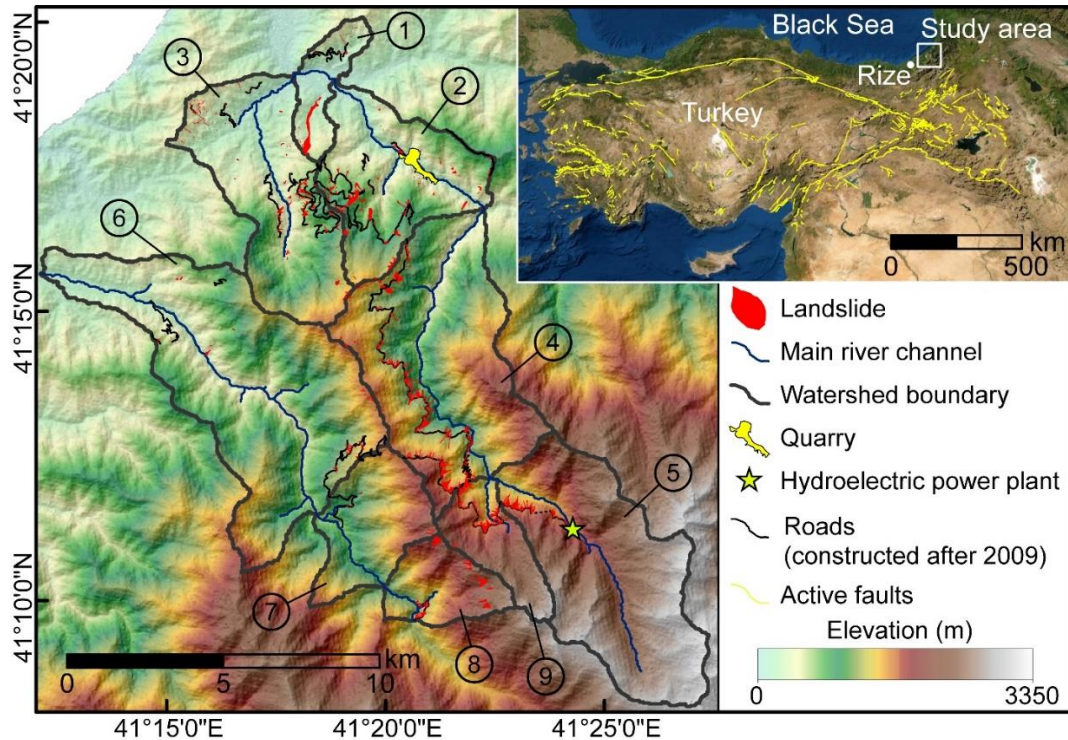
62 As a result, we observe an increasing number of slope failures in seismically active mountain
 63 ranges such as the Himalayan region because of road construction (e.g., Froude & Petley, 2018;
 64 D. N. Petley et al., 2007). However, capturing the anthropogenic effect in landslide occurrence
 65 may not be a trivial task in such environments because seismicity disturbs rock masses and
 66 increases landslide susceptibility irrespective of road construction (e.g., Owen et al., 2008; Tang,
 67 Zhu, Qi, & Ding, 2011). Therefore, differentiating the signal of anthropogenic effect from the
 68 seismic one can be a challenge in some cases. For instance, Khattak et al. (2010) and Khan et al.
 69 (2013) examine the post-seismic landslide evolution following the 2015 Kashmir earthquake and
 70 emphasize the possible confusion between landslides triggered by road construction and strength
 71 reduction caused by seismic shaking. The same difficulty distinguishing the contribution of
 72 anthropogenic and seismic factors in landslide occurrence can also be valid for slope failures that
 73 occurred following the 2015 Gorkha earthquake. Jones et al. (2020) report an increased landslide
 74 rate from 2016 to 2018, which is argued to be primarily associated with the increase in road-
 75 construction efforts. However, the disturbance induced by the earthquake is inevitably a part of
 76 the predisposing factors.

77 This implies that capturing the anthropogenic effect could be more convenient in an environment
78 at which seismicity does not play a significant role in landslide occurrence. Therefore, in this
79 study, we focus on a mountainous area located in the northeastern part of Turkey, where the site
80 has been exposed to no significant seismicity but to multiple road construction projects. We
81 examine not only expanding roads, but also mass movements associated with those roads over
82 the last 10 years. To assess the role of the anthropogenic effect, we also map landslides that do
83 not show any direct relation with roads. Ultimately, we compare our landslide inventory
84 triggered by hillslope cutting and a landslide inventory associated with an earthquake, which is
85 one of the most common triggers (D. Petley, 2012). By this comparison, we aim to better assess
86 how relevant human influence can be compared to natural processes.

87 **2 Study area**

88 The study area is located in the northeastern part of Turkey within the municipal boundaries of
89 Findıklı, Rize, and Arhavi, Artvin. It comprises nine catchments over approximately 195 km²
90 (Fig. 1). Volcanics and volcanoclastics are the main geological units seen in the study area
91 (MTA, 2002). Specifically, the alternation of basalt-andesitic lava, pyroclastics, sandstone, marl,
92 and clayey limestone has been observed throughout the area (Alan et al., 2019).

93 The study area extends approximately 25 km from the coastline and within the zone, elevation
94 sharply increases to 3350 m from the sea level. This reflects the steep topography in the area.
95 The maximum slope steepness within the examined area is 72°, whereas the average slope
96 steepness is 29°±11°.

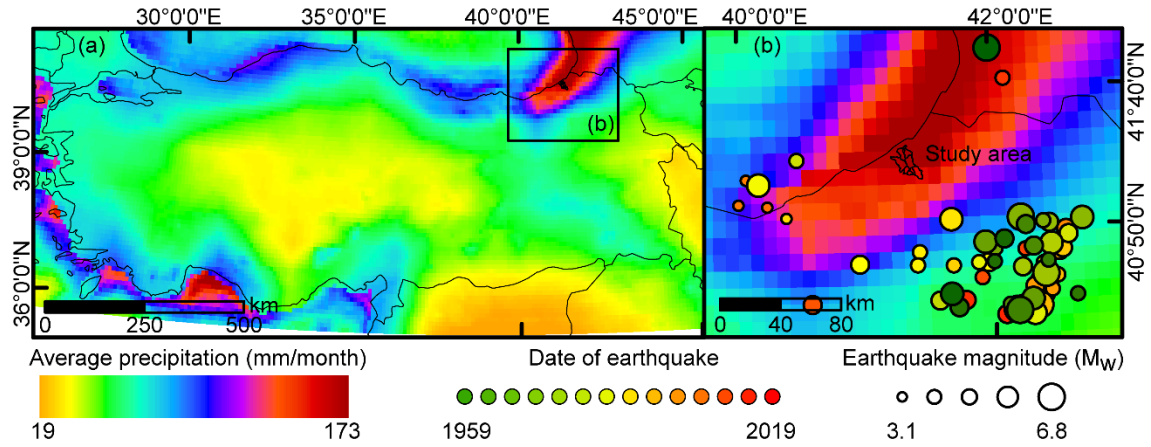


97
98

Figure 1. Overview of the study area. Catchments are labelled by numbers.

99 The steep topographic features of the site are coupled with a strong precipitation regime. The
 100 study area is within the zone receiving the highest precipitation measured throughout Turkey
 101 (Fig. 2a). Based on the 20 years (from 2000-06-01 to 2020-03-31) time series of the Integrated
 102 Multi-Satellite Retrievals (IMERG) Final Run product (Huffman, Stocker, T, Nelkin, & Tan,
 103 2019), which is available through Giovanni (v.4.32) (Acker and Leptoukh, 2007) online data
 104 system, the average monthly precipitation of extreme events (i.e., above 0.95 quantile) is 353 ± 40
 105 mm/month. The same dataset also shows that the average daily precipitation of extreme events is
 106 39 ± 17 mm/day.

107 As for the seismicity, the study area has not been exposed to strong external forces caused by
 108 earthquakes. It is approximately 270 km from the North Anatolian Fault Zone (Fig. 1). The
 109 Earthquake catalog of U.S. Geological Survey (2017) shows that in the last 100 years no
 110 earthquake ($M_w > 3$) occurred within a buffer zone of 50 km radius centered within the study area
 111 (Fig. 2b). The largest earthquake ($M_w = 6.8$) occurred in 1983, approximately 120 km southeast of
 112 the study area. Except for this event, only seven earthquakes of magnitude larger than 5.0 have
 113 occurred in the near vicinity and the closest epicentral location is 70 km away from the study
 114 area.



115

116 **Figure 2.** Maps showing the characteristics of the study area regarding (a) the precipitation
 117 amounts that is the highest of entire Turkey (Huffman et al., 2019) and (b) the seismic record of
 118 the area for earthquakes occurred after 1900 (U.S. Geological Survey, 2017).

119 Although the site has not been exposed to strong seismicity, landslides are one of the main
 120 natural hazards threatening the East Black Sea region and extreme precipitation, land-use change
 121 and road construction are the most common factors causing landslides (e.g., Nefeslioglu,
 122 Gokceoglu, Sonmez, & Gorum, 2011; Raja, Çiçek, Türkoğlu, Aydın, & Kawasaki, 2017; Reis,
 123 Nişancı, & Yomralioğlu, 2009). During the last decade, an increasing number of road
 124 construction projects has been increasing the landslide susceptibility in the Black Sea Region
 125 (e.g., Raja et al., 2017). In particular, within our study area, road constructions have a significant
 126 role in landslide occurrences (Akbulut & Kurdoglu, 2015). Road construction has been
 127 conducted for three main reasons: (1) to increase the accessibility to highlands to boost tourism
 128 in the region (*Green Road project*, DOKAP, 2014), (2) to build a hydroelectric power plant
 129 (HEPP) in the southern part of the study area and (3) to improve the road network overall. Some
 130 of the roads constructed under the third category could be indirectly associated with the first two
 131 classes because newly constructed roads may have further stimulated the construction of others.

132 These construction projects are met with resistance from both non-governmental environmental
 133 organizations (e.g., WWF, 2020) and geoscientific community (e.g., Akbulut & Kurdoglu, 2015)
 134 because the study area is within the Caucasus ecoregion, which is one of the world's 34
 135 biodiversity hotspots (Şekercioğlu, Anderson, Akçay, Bilgin, et al., 2011). The Kamilet Valley
 136 crossing through the study area (Sub-basins 4, 5 and 9 in Fig. 1) is one of the sites reflecting the
 137 rich biodiversity of the region. It hosts numbers of endemic and rare non-endemic plants species
 138 that need to be protected (Akbulut & Kurdoglu, 2015; Şekercioğlu, Anderson, Akçay, & Bilgin,

139 2011; Yuksel & Eminagaoglu, 2017). Therefore, the research question of this study -- that aims
140 at exploring the anthropogenic control on hillslope erosion processes -- also has implications on
141 the protection and sustainable development of a biodiversity hot spot.

142 **3 Materials and method**

143 We map both landslides and constructed roads from 2010 to June 2020. To create these multi-
144 temporal inventories, we use PlanetScope (3-5 m), Rapid Eye (5 m) images acquired from Planet
145 Labs (Planet Team, 2017) and high-resolution Google Earth scenes. The details of the satellite
146 images we used are presented in Table S1.

147 We create inventories based on the systematic examination of satellite images through manual
148 mapping. We always compare two images to map landslides that occurred and roads that were
149 constructed within the examined time window. We do not follow a fixed temporal resolution to
150 map landslides or roads. In fact, we aim at using all the available cloud-free satellite images.
151 Thus, the resulting temporal resolution of the landslide inventories is not fixed and actually
152 increases after 2016, following the increase in the number of available images. For instance, the
153 temporal resolution of our inventory is approximately one year between 2010 and 2011, whereas,
154 after 2016, it is much finer at up to one-month frequency (Table S1).

155 While mapping, we examine whether or not landslides are associated with road construction. For
156 this binary labelling, we manually go through the inventory and identify the ones having contact
157 with roads. If the target landslide crosses a road or is initiate right under a road cut, we label the
158 given landslide as a human-induced one.

159 Also, we group landslides that occurred and roads that were constructed based on two different
160 criteria, namely, by assigning a label describing the purpose of road construction and the
161 occurrence/construction time. For the former one, we examine the purpose of road constructions
162 and categorize them under three headings: (1) HEPP project, (2) Green Road project and (3)
163 others (i.e., roads constructed after 2010 for other reasons than Green road and HEPP projects).
164 Using the same classification, we label not only roads but also the corresponding landslides. We
165 also compare landslides associated with road constructions and the ones triggered by
166 precipitation. We do so by examining the occurrences of landslides for different catchments.

167 This allows us to better investigate the anthropogenic influence by comparing two adjacent
 168 catchments exposed to different levels of external disturbances caused by road construction.

169 For the second criterion, we label landslides/roads using one year of fixed temporal windows. As
 170 a result, we create 11 temporal categories that we can use to examine the evolution of both
 171 landslides and roads from 2010 to June 2020 with one year temporal resolution. We do not
 172 differentiate source and depositional areas of landslides and delineate them as a part of the same
 173 polygon. If the existing landslides expand over time, we only map the new surface in the
 174 examined time window.

175 To examine the landscape characteristics and precipitation regimes, we use Shuttle Radar
 176 Topography Mission (SRTM) digital elevation models (approximately 30-m resolution) (NASA
 177 JPL, 2013) and the Global Precipitation Measurement (GPM), the Integrated Multi-Satellite
 178 Retrievals (IMERG) Final Run product (Huffman et al., 2019).

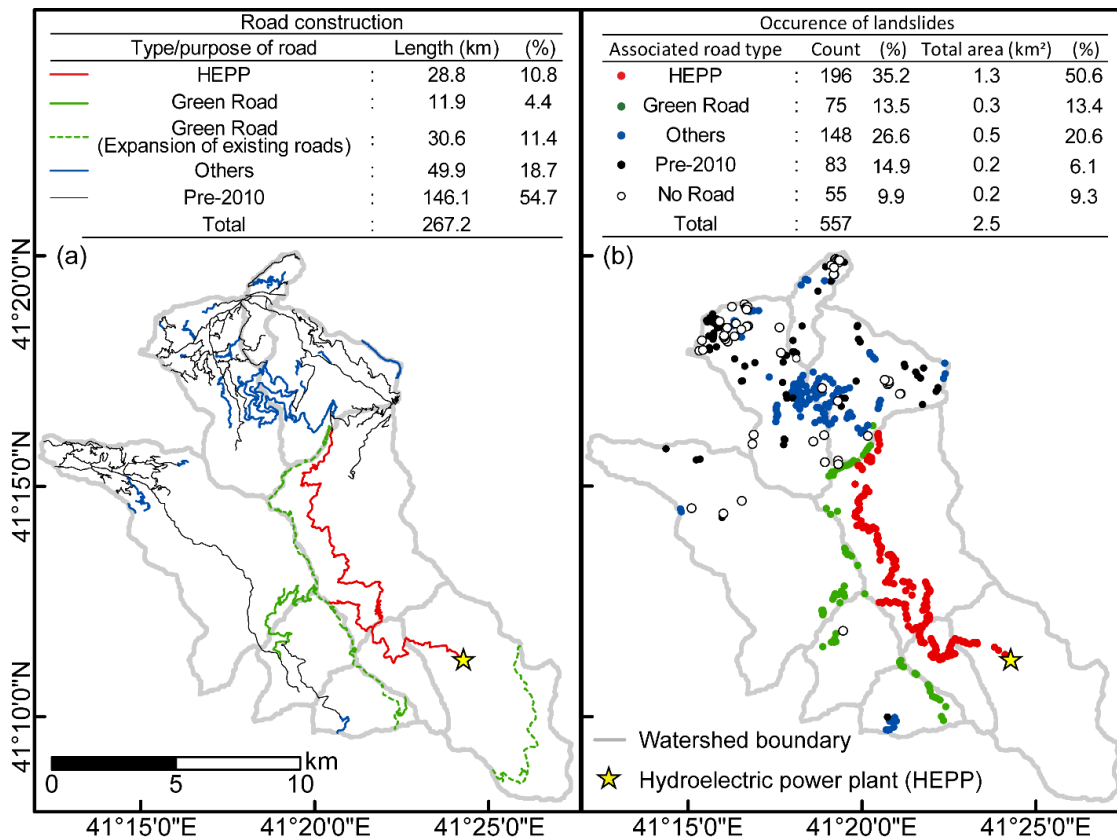
179 Ultimately, we compare our human-induced mass movement inventory with a sample of
 180 earthquake-induced landslide inventories, available via the U.S. Geological Survey ScienceBase
 181 platform (Schmitt et al., 2017; Tanyaş et al., 2017). We make this comparison to assess how
 182 hazardous road construction could be compared to naturally occurring landslides. For the
 183 comparison, we examine the landslides' size statistics, which has been used as a basis to identify
 184 landslide-event magnitude scale (mLS) and provides a measure to quantify the severity of
 185 landslide events (Malamud, Turcotte, Guzzetti, & Reichenbach, 2004). We calculate mLS using
 186 the code provided by Tanyaş et al. (2018). We also calculate the slope of the power-law
 187 distribution (β , power-law exponent) that the frequency-density distribution of landslides
 188 exhibits (e.g., Guzzetti, Malamud, Turcotte, & Reichenbach, 2002; Malamud et al., 2004;
 189 Tanyaş, van Westen, Allstadt, & Jibson, 2019) using the method proposed by Clauset et al.
 190 (2009). To estimate an earthquake magnitude for an equivalent earthquake-induced landslide
 191 inventory with our human-induced one, we use the empirical relation between earthquake
 192 magnitude (M) and landslide-event magnitude scale (Malamud et al., 2004).

193 $mLS=1.29 \times M-5.65$ (1)

194 **4 Results**

195 **4.1 Mapping of roads and landslides**

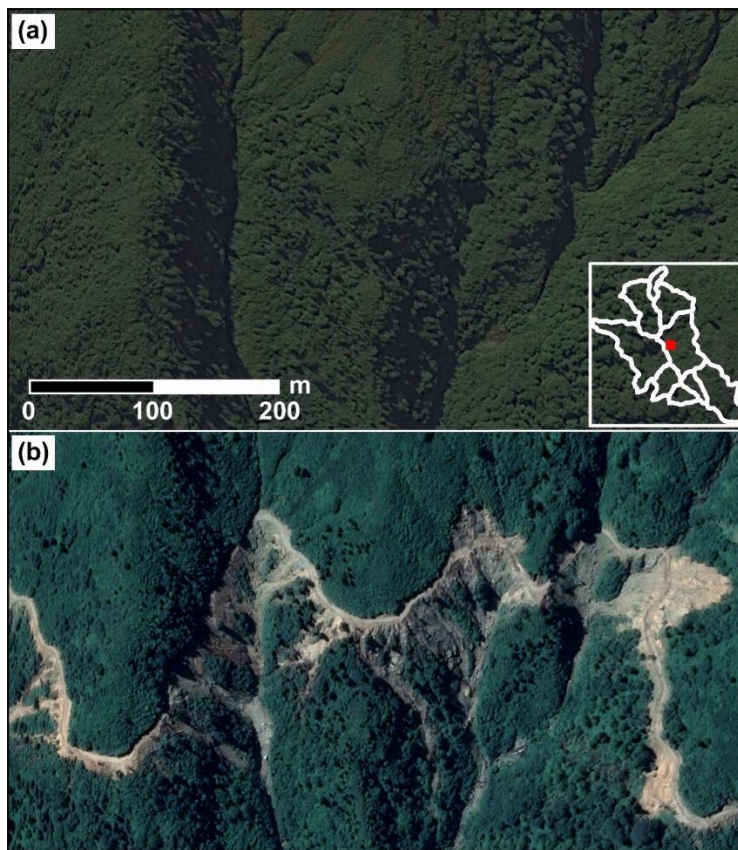
196 We identified the roads associated with “HEPP” and “Green Road” projects (Fig. 3a) based on
 197 information from our local contacts and interviewees. They informed us about other expansion
 198 work conducted along the route of the Green Road project. We could not identify the time of
 199 these expansions, but we know the sections where the engineering work was carried out. We
 200 labelled the roads that already exist as of January 2010 as “Pre-2010” based on our analyses of
 201 satellite scenes. We labelled the rest of the roads constructed after 2010 as “Others”. Based on
 202 the identified roads, we also labelled corresponding mass movements (Fig. 3b).



203
 204 **Figure 3.** Maps showing the distribution of (a) the roads constructed for different purposes and
 205 (b) the associated landslides.

206 To create these road and landslide inventories, first, we mapped both roads and landslides
 207 associated with HEPP (Fig. 3). Mapping landslides was particularly challenging because of the
 208 short-term interactions between mass movements and engineering activities. Specifically, local
 209 people indicated that the excavated hillslope materials were mostly dumped into the river
 210 channels during the construction, and also down the slope of the road cut. This may have also
 211 induced some landslides further down the hillslope because of the additional load. Notably, this

212 makes the identification of landslides difficult because the dumped hillslope materials and
 213 landslides triggered by the construction are mostly mixed and have a similar appearance in
 214 satellite scenes. For instance, Figure 4 shows a segment of the road excavation conducted as part
 215 of the *HEPP* project. This satellite image clearly shows that dumped materials are mixed with
 216 landslides triggered by road construction. We can both see mass movements that were initiated
 217 from the upper or lower hillslopes. For the former ones, we can be sure that these are human-
 218 induced landslides. However, for the latter cases, we cannot differentiate whether they are solely
 219 dumped materials or human-induced landslides. In fact, most likely, their genesis is the result of
 220 the coupled effect of both processes.



221
 222 **Figure 4.** Satellite scenes showing the pre- and post- excavation landscape in a selected area (41°
 223 $13' 56''$ N and $41^{\circ} 20' 18''$ E) along the route excavated for the *HEPP* project. The examined
 224 segment of the road was constructed between 17th July 2016 – 6th September 2016. Within the
 225 same period, mass movements widely occurred. We also identified some landslides enlarged
 226 between 6th September 2016 – 9th July 2017. The location of the sample area is geographically
 227 shown in the lower right of the panel (a).

228 Local interviews also emphasized that the road construction carried out for the *HEPP* project has
 229 dramatically affected the natural course of erosional processes since 2016 (Fig. 5). They argue
 230 that explosives were used in some parts of the road construction to facilitate the progress of the
 231 project. This most likely weakened the shear strength of hillslope material, increasing the
 232 landslide susceptibility of the given site and promoting the failures we noted.



233
 234 **Figure 5.** Photos showing the mass movements on hillslopes associated with road constructions
 235 of *HEPP*. The photos were taken on 15th June 2020 (Photographs courtesy of Hasan Sıtkı
 236 Özkazanç).

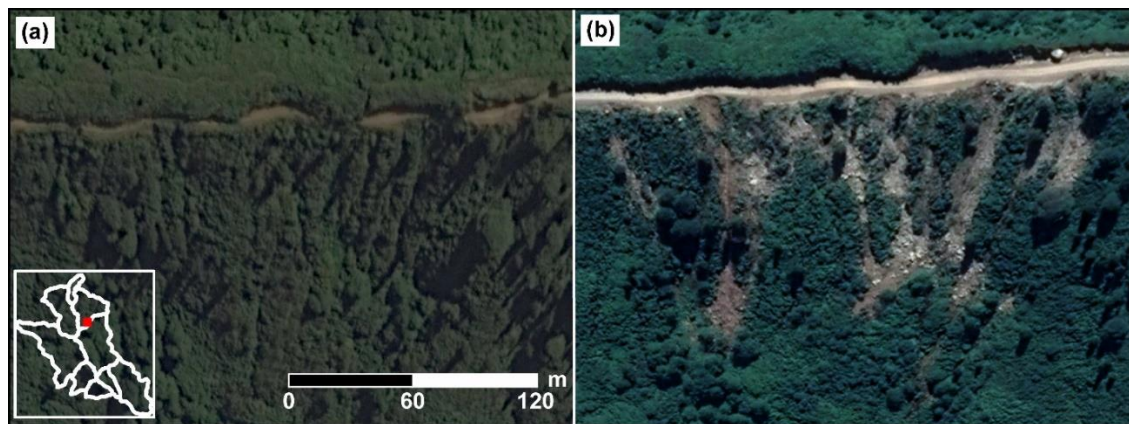
237 Overall, the differentiation between dumped materials and human-induced landslides is
 238 challenging. Regardless, these processes initiate additional anthropogenic sediment loads to
 239 river channels. The local environmental organizations (*Arhavi Doğa Koruma Platformu*)
 240 provided evidence to this claim in an early 2020 report where an increased sediment content was
 241 noted in the Kamilet River (Fig. 6). Therefore, in this study, we did not differentiate the dumped
 242 hillslope materials and landslides; instead, we considered them all as human-induced mass
 243 movements.



244

245 **Figure 6.** Photos showing the intersection of Kamilet and Durguna Rivers ($41^{\circ} 16' 34''$ N and 41°
 246 $22' 32''$ E) where increased sediment content in Kamilet River caused by the *HEPP* construction
 247 is evident. The pictures were taken in May 2020. Location of this spot is given in the lower right
 248 of the panel (b) (Photos by Hasan Sıtkı Özkazanç).

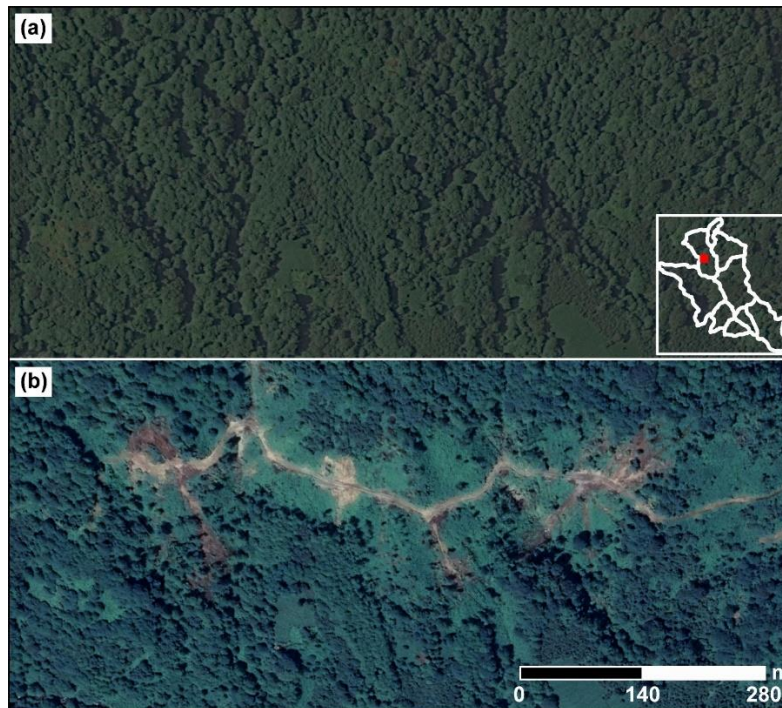
249 We also mapped mass movements that occurred along with the Green Road project (Fig. 3).
 250 Some of the mass movements occurred along existing roads, which were expanded in relation to
 251 the Green Road project. Similar to the *HEPP* case, dumped hillslope materials might also play a
 252 role in these mass movements. However, Figure 7 shows that the crests of some mass
 253 movements extend backward from the road and therefore, we argue that these must be a mixture
 254 of both dumped materials and human-induced mass movements if they are not purely human-
 255 induced mass movements.



256

257 **Figure 7.** Google Earth scenes showing the pre- and post- expansion landscape at a selected site
 258 ($41^{\circ} 15' 37''$ N and $41^{\circ} 20' 24''$ E) along the route excavated for the Green Road project. Mass
 259 movements occurred between 18th September 2017 – 27th May 2018. The location of these mass
 260 movements is given in the lower left of panel (a).

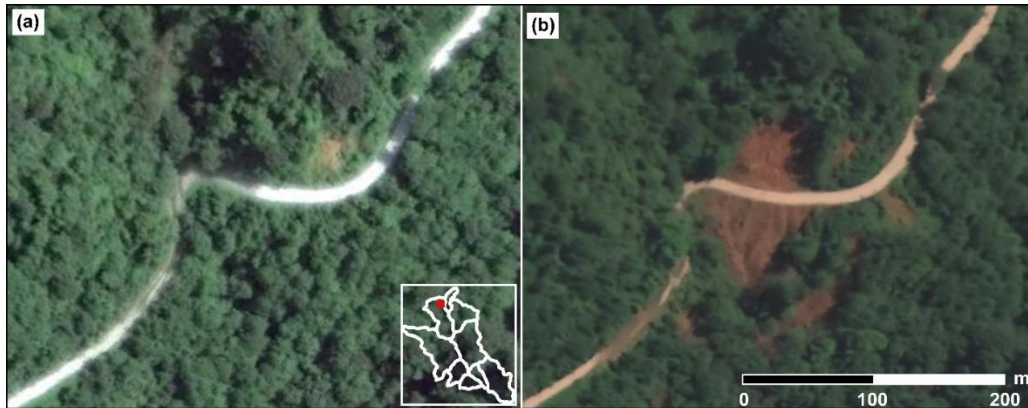
261 Moreover, we mapped mass movements that occurred along other roads (i.e., *Others*) that were
 262 excavated during the same period (Fig. 3). These are mostly secondary and private roads opened
 263 to access agricultural sites or houses and therefore, they were created without the use of
 264 explosive. Consequently, excavated materials are expected to be less compared to HEPP and
 265 Green Road, which were designed for higher traffic loads that require a wider road section and
 266 cut. Figure 8 shows an example of human-induced mass movements along roads labelled as
 267 *Others*.



268
 269 **Figure 8.** Google Earth scenes showing the pre- and post- road expansion conditions at a
 270 selected site ($41^{\circ} 16' 24''$ N and $41^{\circ} 17' 51''$ E) representing the mass movements categorized as
 271 *Others*. The examined the segment of the road constructed between 10th September 2013 – 3rd
 272 September 2014. Landslides occurred between 18th November 2017 – 27th May 2018 and 20th
 273 March 2019 – 21st May 2019. The location of these mass movements is given at the lower right
 274 of the panel (a).

275 Ultimately, we mapped landslides that occurred along the existing roads (*Pre-2010*) (Fig. 9) and
 276 the ones triggered by natural agents irrespective of roads (*No Road*) (Fig. 10). Precipitation is the
 277 most likely triggering factor for these landslides. However, for the Pre-2010 case, road works
 278 should have played a crucial role in the failure mechanism by disturbing both resisting forces

279 against sliding and hydrological conditions. As for the *No Road case*, in addition to precipitation
 280 as a triggering factor, some anthropogenic factors might have played a role, albeit to a much
 281 lesser extent. We will elaborate on the possible contribution of those indirect anthropogenic
 282 factors in Section 5.



283
 284 **Figure 9.** Google Earth scenes showing the pre- and post- landslide views at a selected site (41°
 285 $18' 20''$ N and $41^{\circ} 20' 14''$ E), representing the mass movements that occurred along an existing
 286 road (i.e., *Pre-2010*). Mass movements occurred between 3rd November 2016 – 16th April 2017.
 287 The location of these mass movements is given in the lower right of the panel (a).



288
 289 **Figure 10.** Google Earth scenes showing the pre- and post- landslide landscape at a selected site
 290 ($41^{\circ} 18' 20''$ N and $41^{\circ} 17' 58''$ E) representing the mass movements triggered by natural agents

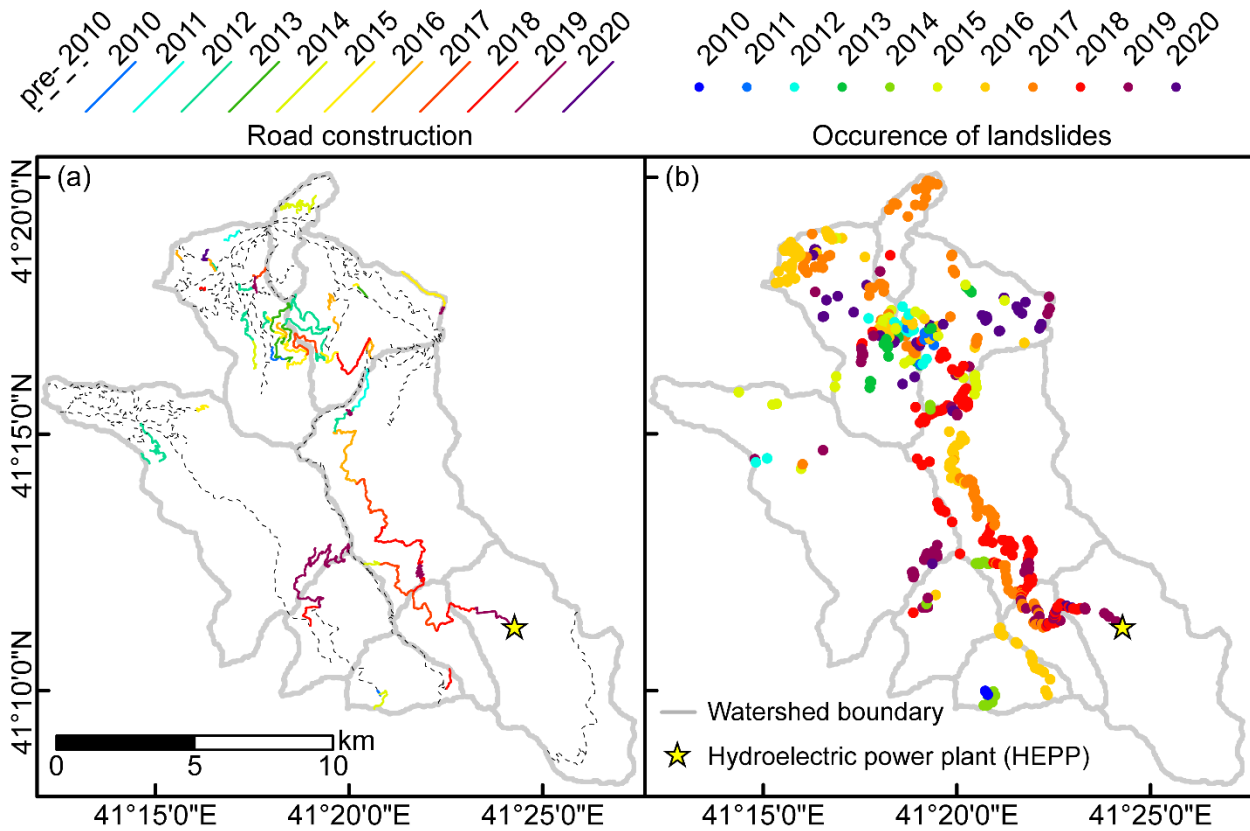
291 (i.e., *No Road*). The landslide occurred between 17th July 2016 – 9th September 2016. The
 292 location of the landslide is given in the lower left of the panel (a).

293 **4.2 Analyses of mass movements**

294 We mapped 557 mass movements and a 267.2 km long road network. Overall, 33.9% of the
 295 roads were developed during the last 10 years, for various purposes (see Fig. 3a). Among them,
 296 10.8% is associated with the *HEPP* project and 4.4% is related to the *Green Road* project. Also,
 297 some of the existing roads have been extended in relation to the *Green Road* project and this
 298 contribution refers to 11.4% of all roads in the study area. Moreover, 18.7% of the roads
 299 constructed after 2010 are not directly associated with the *HEPP* nor the *Green Road* projects,
 300 but some indirect connections could exist (*Others*).

301 We also examined mass movements in relation to road work. Our findings show that 90.1% of
 302 them occurred after 2010 while being in immediate proximity to the roads (Fig. 3b). As for the
 303 cumulative area of mass movements, the anthropogenic influence is also significant: 90.7% of
 304 total size is associated with road constructions. Roads constructed as part of the *HEPP* project
 305 has the most substantial contribution to mass movements occurrences. In the study area, 1.3 km²
 306 of mass movements were solely caused by the *HEPP* project, which refers to 50.6% of the total
 307 size identified in the study area. During the last 10 years, 9.9% of landslide occurred with no
 308 direct relationship with roads. In terms of total size, the influence of these landslides constitutes
 309 9.3% of the total area of mass movements. This static summary is complemented below by
 310 examining the variation in both road construction and landslide occurrence on a temporal basis
 311 (Fig. 11 and 12). We noticed a peak value in road construction in 2012. However, the peak in the
 312 constructions does not correspond to a significant number of landslides. This is mainly because
 313 of the morphologic conditions encountered through the route. In fact, most of the roads we
 314 mapped between 2011 and 2012 are associated with roads categorized as *Others*. The mean slope
 315 steepness observed through these roads is 23°, which is lower than mean steepness encountered,
 316 for instance, through the roads associated with the *HEPP* project (33°) (Fig. 12). This is also the
 317 case for two other categories (i.e., *Pre-2010* and *Green Road*). They both cross relatively smooth
 318 topography compared to the *HEPP* project. Specifically, the *Green Road* project mainly follows
 319 the existing old road path, which passes through ridges (Fig. 3a). Therefore, a predominant part
 320 of these roads did not require any hillslope cut in our study area. This explains why the mass

321 movements triggered in response to the activities of the *HEPP* project gave the largest damage
 322 among different construction projects (Fig. 3b).

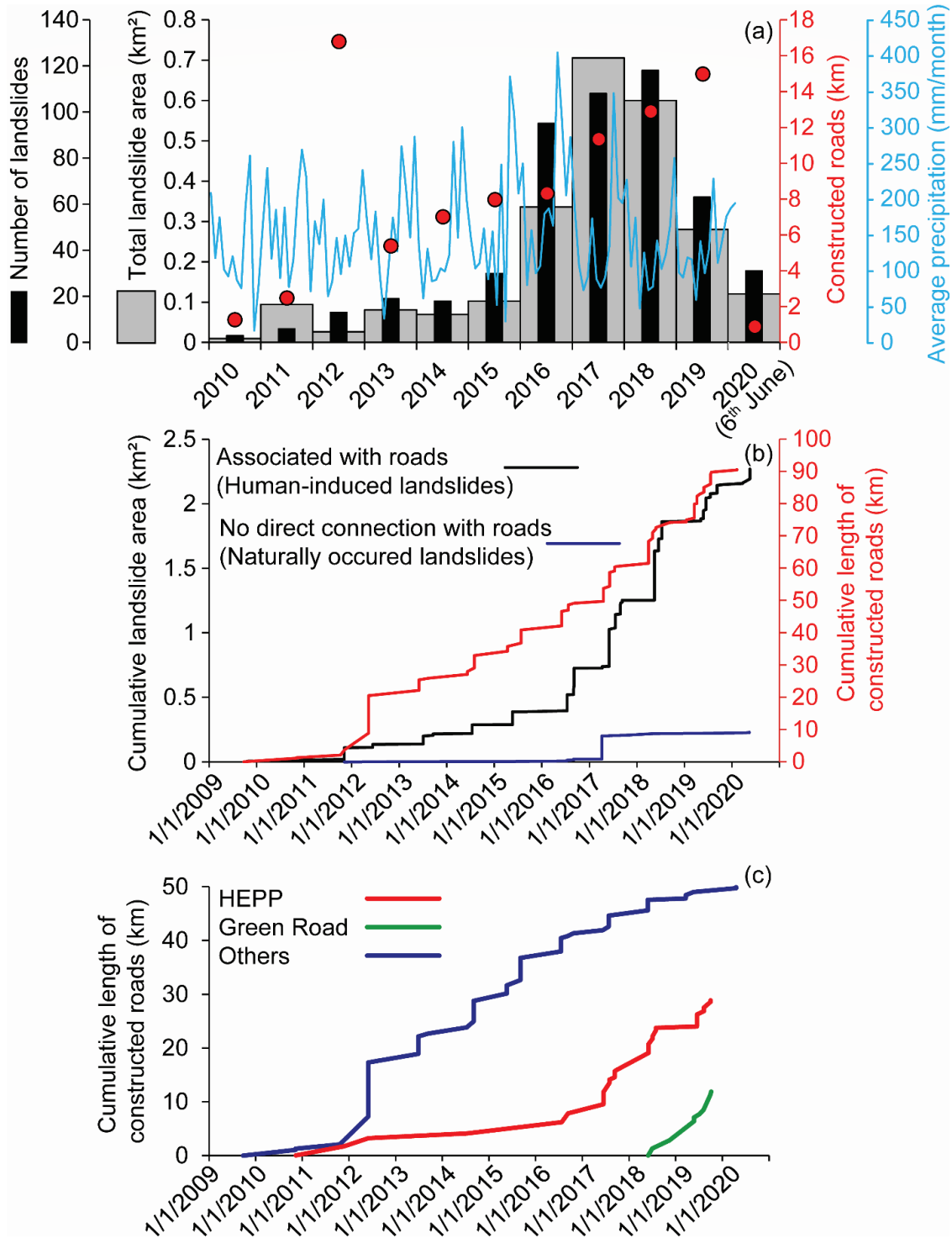


323
 324 **Figure 11.** Maps showing the temporal evolution of (a) the roads and (b) the associated
 325 landslides.

326 After 2016, the total length of constructed roads per year increases (see, Fig. 12a). As a result,
 327 the number of landslides associated with road construction also significantly increases after
 328 2016. Since then, the contribution of naturally triggered landslides becomes negligible (Fig.
 329 12b).

330 In 2016, an increase in the landsliding trend could also be linked to strong precipitation (average
 331 monthly precipitation was approximately 200 mm/month in 2016). However, in the following
 332 years, landslide rates are still higher than pre-2016 levels, although the amount of precipitation is
 333 equal or less than the pre-2016 levels (<150 mm/month). These findings indicate that the
 334 increase in landslide rate is mostly due to road constructions regardless of extreme rainfall
 335 events.

336

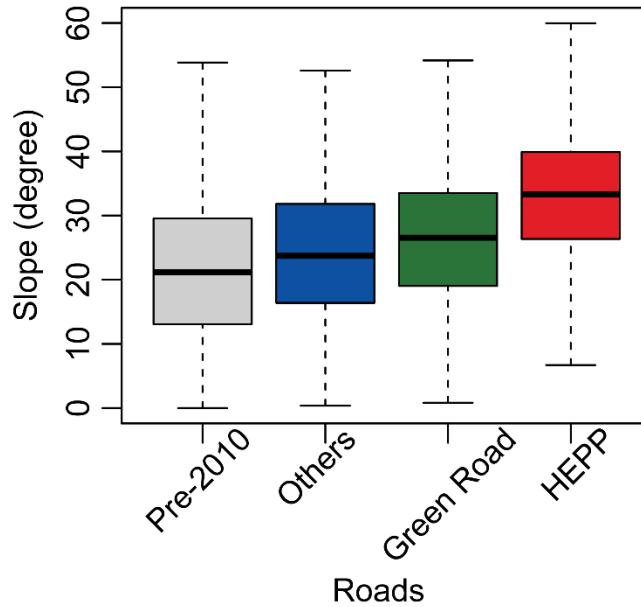


337

338 **Figure 12.** Plots showing the yearly variation in road constructions and landslide occurrences

339 from 2010 to 2020. (a) The number and the total area of landslides against the entire length of

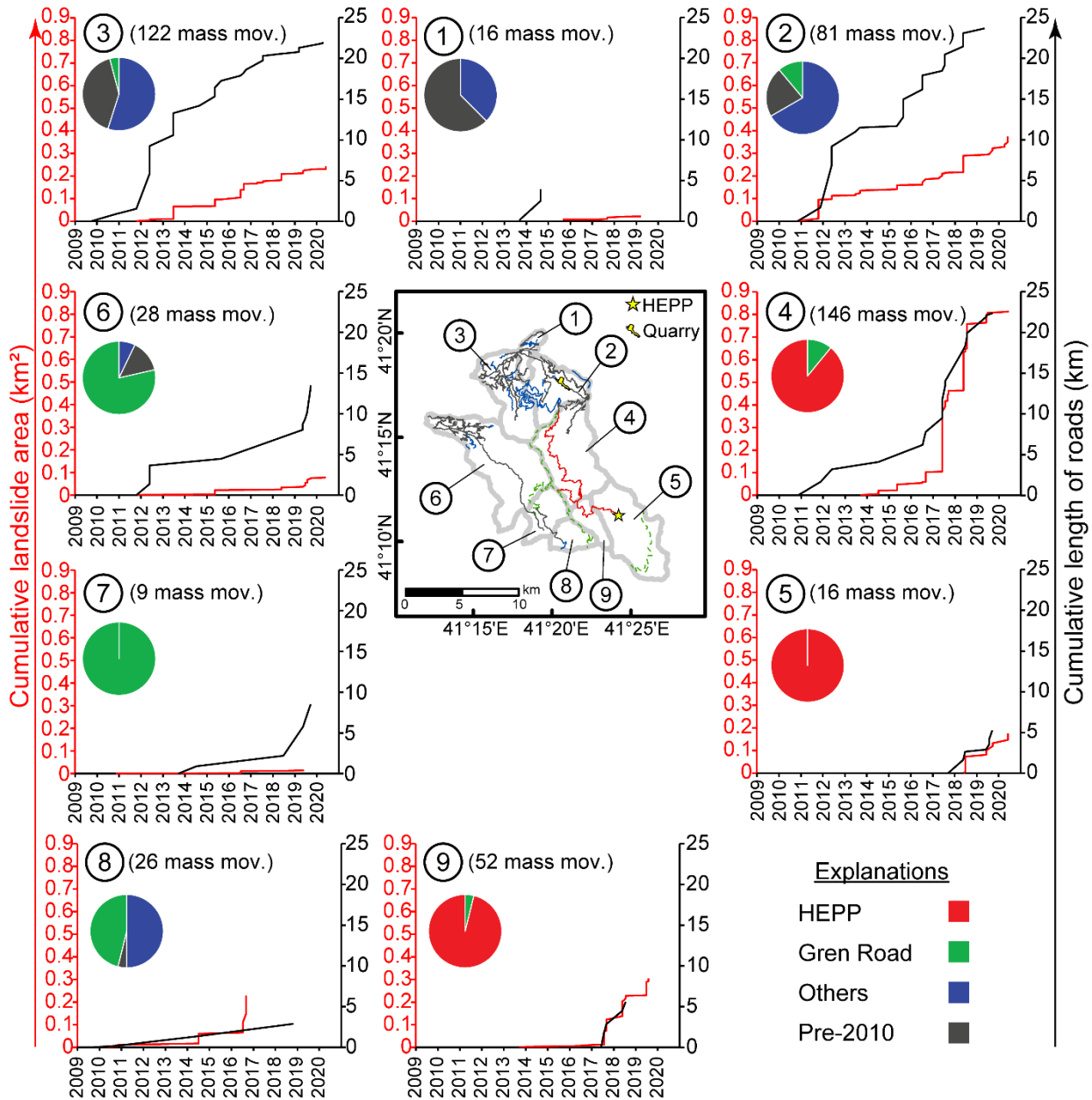
340 constructed roads. (b) The cumulative trend in total landslide size and road length and (c) the
 341 roads constructed for different purposes.



342
 343 **Figure 13.** Boxplots showing the range of slope steepness along roads constructed for different
 344 purposes.

345 We also examined how the road constructions evolved after 2010 in each catchment and,
 346 consequently, how this affected the occurrences of mass movements per hydrological unit.
 347 Figure 14 shows the summary of this temporal evolutions. For this analysis, we excluded the
 348 naturally occurring landslides. Our findings show that if there is no significant road construction,
 349 the number of mass movements is relatively low. For instance, catchments 1, 2, 3 and 4 are
 350 adjacent catchments. Among them, catchment 1 is the only hydrological unit where the total
 351 length of constructed roads in the last 10 years is less than 5 km. The associated total landslide
 352 size in catchment 1 is 0.02 km², whereas, in the three other catchments (2,3 and 4), it ranges
 353 from 0.24 km² to 0.82 km². We observed a similar situation in catchments 5, 8 and 9, where we
 354 identified a relatively low amount of road constructions (<~5 km) associated with a limited
 355 number of landslides (Fig. 14). In catchments 6 and 7, the total length of the road (~10 km) is in
 356 between two other sets we mentioned above, but we identified 28 and 9 landslides in these
 357 catchments. These roads are mostly associated with the *Green Road* project and thus the limited
 358 number of landslides is most likely because of the steepness of the route followed during the
 359 construction (Fig. 13).

360

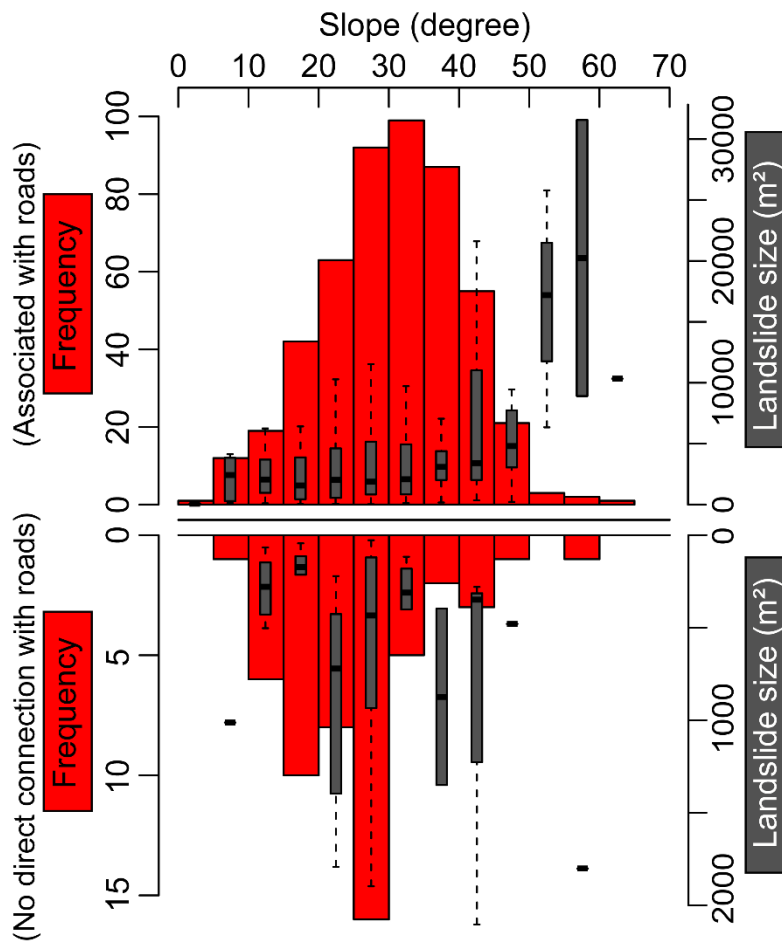


361

362 **Figure 14.** Figure showing the temporal evolution of both roads and landslides within each
 363 catchment from 2010 to June 2020. Catchments 2, 3 and 4 appear as hydrological units exposed
 364 to the highest road construction and consequently, the largest number of mass movements.

365 We also compared human-induced landslides with naturally occurred ones in terms of slope
 366 steepness and size of landslides. Figure 15 shows that slope steepness of human-induced
 367 landslides varies quite broadly compared to naturally occurred landslides. Hillslopes where the

368 slope steepness ranges from 15° to 50° are associated with a minimum of 20 and a maximum of
 369 100 human-induced landslides. Conversely, the frequency of naturally occurring landslides
 370 increases up to 30° (with a minimum of five and a maximum of 15 landslides), and then sharply
 371 decreases for steeper slopes. This large difference is undoubtedly induced by road excavations
 372 performed on steep slopes, as demonstrated by the much more numerous mass movements that
 373 occurred under anthropic disturbance. In fact, the same slope ranges appear to be mostly stable
 374 under natural conditions. Also, there is a large difference in average landslide size triggered by
 375 road constructions and natural agents. The average size of human-induced landslides is
 376 approximately ~20,000 m² in the steepest slopes (i.e., 55°-60°), whereas the maximum average
 377 size of naturally occurring landslides is ~1000 m².



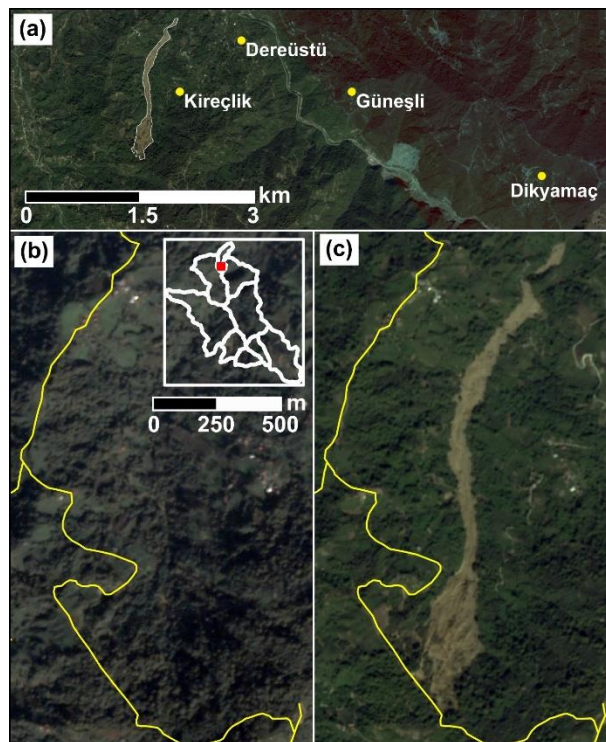
378
 379 **Figure 15.** The comparison of human-induced landslides (top panel) with naturally occurred
 380 (bottom panel) ones in terms of slope steepness and landslide size characteristics.

381 **5 Discussion**

382 In this study, we provide quantitative, thorough systematically mapping mass movement rate
383 after major road constructions in a mountainous region that is exposed to strong precipitation
384 regimes. We specifically chose this region because seismicity does not play an active role here
385 and therefore, capturing the anthropogenic effect on slope stability is more evident than in
386 tectonically active mountainous regions such as Nepal, India or Pakistan. In tectonically active
387 areas, the legacy of previous earthquakes could last for a long period, increasing the landslide
388 susceptibility (R. N. Parker et al., 2015). In particular, after strong earthquakes, the elevated
389 susceptibility is noticeable in the following years (up to nine years) and it decreases over time
390 (e.g., Fan et al., 2018). Consequently, in such environments, it would be challenging to
391 decompose the signal of earthquake legacy from anthropic disturbances. Precipitation could also
392 add another layer of complexity. In fact, the occurrence of a landslide or a population of
393 landslides is always controlled by multiple predisposing and triggering factors (e.g., geotechnical
394 properties, hydrologic conditions, land cover, external loads, etc.) (e.g., Jaboyedoff et al., 2018).
395 Capturing the relative contribution of each conditional factor requires not only highly detailed
396 temporal landslide inventories -- where we can assess the exact date of occurrence of each
397 landslide -- but also quantitative measurements of the predisposing factors at a given time.
398 Notably, we lack such detailed datasets in this paper, and this is often the case in many landslide
399 susceptibility studies, even when multi-temporal models are built (e.g., Guzzetti et al., 2005).

400 Despite the complexity we faced and the limited temporal information on other controlling
401 factors, we could still investigate whether a relationship exists between slope failures and
402 anthropogenic effect. To address this issue, we made a binary classification distinguishing
403 human-induced and naturally occurring landslides on the basis of satellite images. However, in
404 some cases, this identification was challenging, as well. For instance, the largest landslide we
405 mapped within the region occurred on 7th November 2016, following a strong precipitation event
406 (Ersoy, 2017). This event was a shallow earth-slide flow that affected an area of approximately
407 0.2 km² within the Kireçli village (Fig. 16). Satellite images show that the crest of the landslides
408 is precisely aligned with an existing road. Some parts of the road failed as a result of this
409 landslide (Ersoy, 2017). The complexity in the interpretation arose because this landslide could
410 also be linked to natural landscape evolution processes. In fact, the landslide initiated at the ridge
411 of the slope where the susceptibility is generally higher. Thus, the shallow landslide might have
412 been triggered regardless of the possible influence of the road.

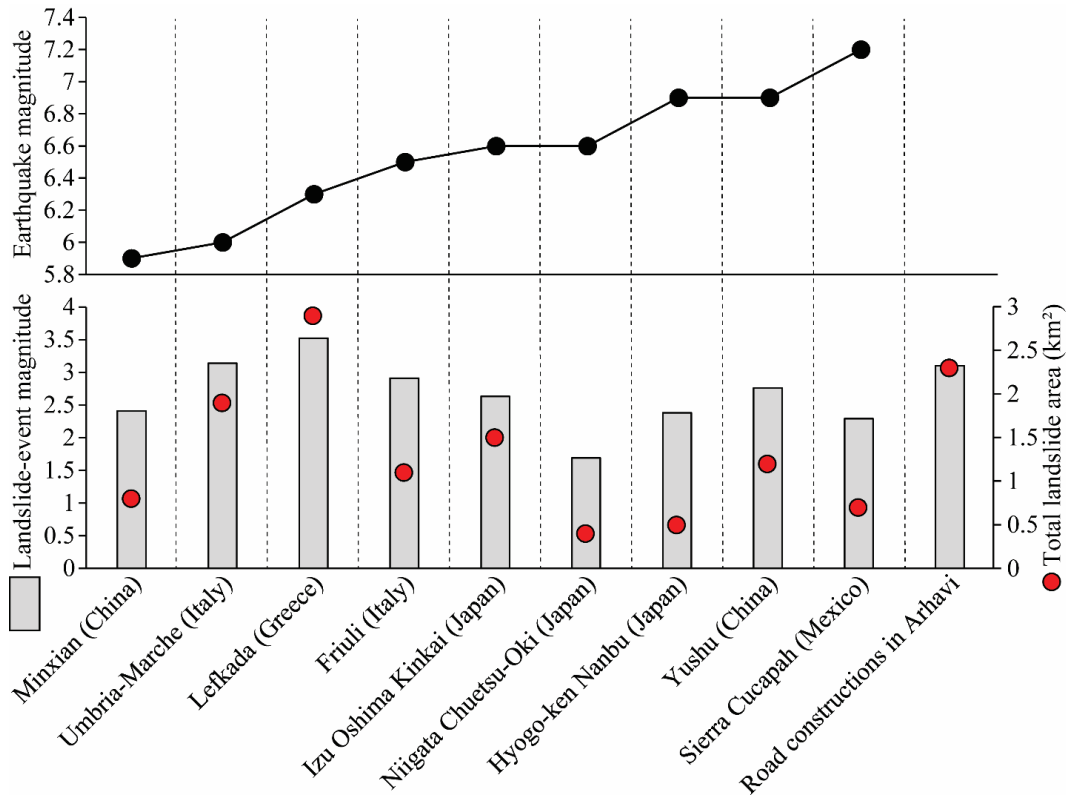
413 In such cases, we labelled landslides as naturally occurring ones since we do not have adequate
 414 support to argue that they are human-induced. We did this to implement a conservative approach
 415 in our analyses. However, emphasis should still be given to the possible direct or indirect
 416 anthropogenic effects. In fact, the road could have a direct implication by increasing the pore
 417 water pressure at the crest of the landslide. Also, the external loads associated with traffic might
 418 be another likely contributor to the landslide initiation. This event is a very interesting example
 419 also because of the existence of an active rock quarry approximately 3 km east. There, to dig into
 420 the slope and collect the material explosives are commonly used. Our local contacts informed us
 421 that some damages had been observed at houses in villages close to the quarry (i.e., Dikyamaç,
 422 Güneşli, Dereüstü villages). Among them, the Dereüstü village is located approximately 2.5 km
 423 northwest of the quarry, at a comparable distance to the mudflow location. Therefore, the
 424 disturbance exerted by activities related to the quarry might have also played a role in triggering
 425 the landslide mentioned above.



426
 427 **Figure 16.** PlanetScope scenes showing the pre- and post- landslide landscape of the largest
 428 landslide mapped within the study area ($41^{\circ} 17' 37''$ N and $41^{\circ} 18' 27''$ E). This landslide
 429 occurred on 7th November 2016. The location with respect to our study area is given in the upper
 430 right of the panel (b). Yellow lines in the panel (b) and (c) indicate roads.

431 A similar anthropogenic effect, if not even stronger, could also be valid for landslides triggered
432 along the roads constructed as part of the *HEPP* project, because of the explosives directly used
433 to cut the hillslope. In fact, apart from hillslope cuts, explosives have been used in the last
434 segment of the road approaching the *HEPP* site. In this section, approximately 620 m of the
435 route passes through a tunnel. In such steep terrain, any time a new road is constructed, the
436 damage to the slope is almost inevitable unless extreme precautions are taken. This is also
437 reported in the literature. For instance, Froude and Petley (2018) report that from 2004 to 2016,
438 30% and 43% of fatal landslides occurred in India and Nepal are associated with road
439 constructions. In these cases, the high landslide rates are not due to the lack of engineering
440 solutions. In fact, landslides triggered in response to road construction projects are a well-known
441 issue for both India and Nepal. The required and appropriate engineering practices necessary to
442 minimize environmental damage have already been documented (e.g., Hearn and Shakya, 2017).
443 The observed landslide hazard associated with road construction is mostly due to neglected
444 engineering solutions (Hearn & Shakya, 2017). Therefore, road construction in mountainous
445 regions should not be envisioned unless the required investment in road design is available
446 (Hearn & Shakya, 2017; Valdiya, 2014). Notably, the site we examined is a good example where
447 road construction has widely damaged the landscape, and it is clear that better precaution or
448 stabilization investments should have been put into practice.

449 To assess the consequences of human effects on mass movements, we also compared our
450 landslide inventory (i.e., only the landslides associated with road constructions) with nine
451 earthquake-induced landslide-event inventories sharing similar landslide-event magnitude and
452 total landslide area. Figure 17 shows that the human-induced mass movement inventory we
453 mapped is compatible with landslide-events triggered by earthquakes having magnitudes varying
454 from $M_w=5.9$ to $M_w=7.2$. This observation is made regardless of climatic and morphologic
455 conditions.



456

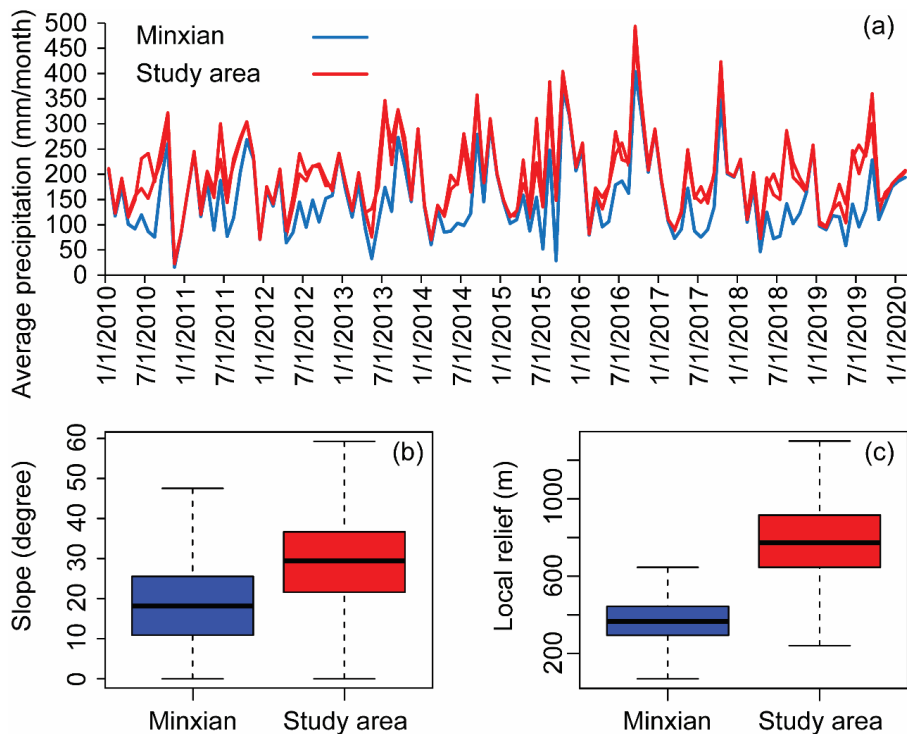
457 **Figure 17.** Comparison between our human-induced mass movement inventory and nine
 458 earthquake-induced landslide inventories. Landslide-event magnitudes were calculated based on
 459 Tanyaş et al. (2018).

460 Among the ten examined cases, the total surface affected by landslides changes significantly
 461 from one case to another, with many cases showing a much larger spatial extent compared to our
 462 study site. Therefore, for a better comparison, we further investigated the landslide inventory
 463 associated with the 2013 Minxian earthquake ($M_s=6.6$ based on the China Earthquake Network
 464 Center and $M_w=5.9$, according to USGS), where the extent of the region affected by landslides is
 465 equivalent to our study area. Specifically, the earthquake occurred between Minxian and
 466 Zhangixan (in the Gansu Province, China) on a thrust fault and triggered 2330 co-seismic
 467 landslides covering $\sim 200 \text{ km}^2$ (Xu, Xu, Shyu, Zheng, & Min, 2014), which is also compatible
 468 with our study area where the examined catchments cover approximately 195 km^2 .

469 The cumulated extent of all the landslide polygons associated with the Minxian earthquake is 0.8
 470 km^2 , whereas the total size of our human-induced landslides is 2.3 km^2 . This shows that even the
 471 mass movements solely related to the *HEPP* project (total landslide area is 1.3 km^2) can
 472 significantly surpass the total co-seismic landslide size induced by the Minxian earthquake.

473 Before comparing the two inventories in terms of their size statistics, we first analyzed in terms
 474 of climatic and morphologic conditions. To collate the climatic information, we used the 20
 475 years (from 2000-06-01 to 2020-03-31) precipitation time series accessed via the IMERG Final
 476 Run product, for both sites. Figure 18a shows that both sites have similar precipitation regimes,
 477 although the precipitation is relatively higher in our study area. Also, slope and local relief
 478 (derived from the SRTM DEM at ~30m) observed in our study area indicate rougher terrain
 479 within the landslide-affected area compared to those affected by the Minxian earthquake (Fig.
 480 18b and 18c).

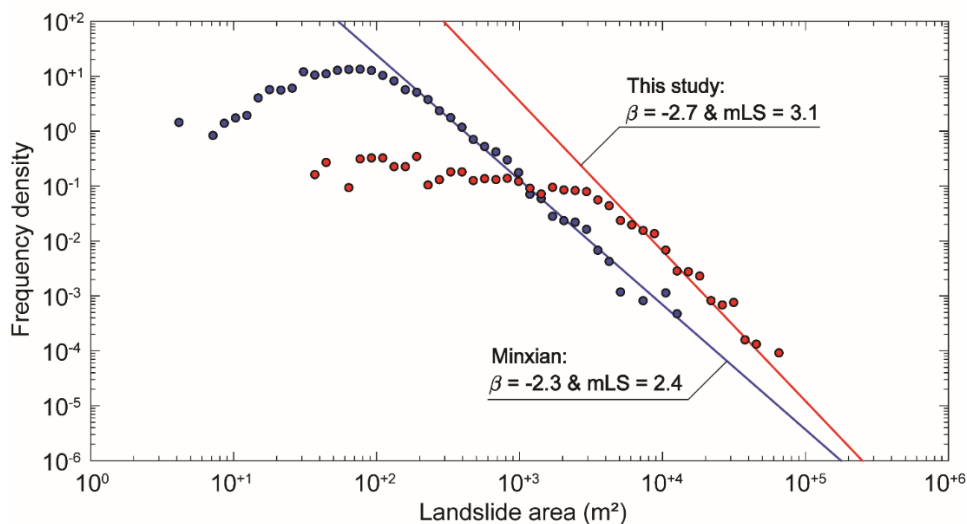
481 We recognize that the two different sites cannot be thoroughly compared because a much more
 482 thorough assessment should be made accounting for detailed
 483 geological/geotechnical/hydrological data. However, on the basis of the simplified overview we
 484 provide, we can hypothesize that if an earthquake with comparable magnitude to Minxian would
 485 occur in our study area, the resultant landslide event should be more significant because our
 486 study area is associated with higher precipitation and steeper terrain conditions.



487
 488 **Figure 18.** Plots comparing our study area with the landslide affected area of 2013 Minxian
 489 earthquake regarding (a) precipitation amounts, (b) slope steepness and (c) local relief.

490 The comparison between the frequency-density distributions of the human-induced landslides we
 491 mapped and those naturally triggered by the 2013 Minxian earthquake shows that larger
 492 landslides were triggered in our Turkish site (Fig. 19). The power-law exponents calculated for
 493 both our inventory ($\beta=-2.7$) and the Minxian inventory ($\beta=-2.3$) are close to each other and align
 494 well with distributions documented in the literature. In fact, power-law exponents of naturally
 495 occurred landslide inventories fall in the range 1.4–3.4, with a central tendency 2.3–2.5 (Stark &
 496 Guzzetti, 2009; Tanyaş et al., 2018; Van Den Eeckhaut, Poesen, Govers, Verstraeten, &
 497 Demoulin, 2007).

498 We also calculated the landslide-event magnitudes of our human-induced landslide inventory
 499 ($mLS=3.1$) and the Minxian inventory ($mLS=2.4$). The difference between the two cases are
 500 consistent with our initial assumption that if a similar earthquake occurred in our study area, it
 501 would be more disastrous. In fact, based on the empirical relation between earthquake magnitude
 502 (M) and landslide-event magnitude scale proposed by Malamud et al. (2004), the earthquake
 503 magnitude for an equivalent earthquake-induced landslide inventory would be 6.8. This shows
 504 how destructive the anthropogenic effect on geomorphological processes could be compared to
 505 natural processes. The destruction produced by the road constructions conducted in the last 10
 506 years is compatible with the possible effect of a theoretical earthquake with a magnitude greater
 507 than 6.0.



508
 509 **Figure 19.** Frequency-density curves plotted for the landslides associated with roads in our study
 510 area (red) and landslide triggered by the 2013 Minxian earthquake (blue). Power-law exponents

511 (β) were calculated based on the method proposed by Clauset et al. (2009), whereas power-law
512 fits and landslide-event magnitudes were identified based on Tanyaş et al. (2018).

513 **6 Conclusions**

514 In this study, we report a distinct correlation of mass movements and major road constructions
515 that explicitly shows human impact on mountainous environments which are under
516 anthropogenic disturbance recently. Our results further suggest that slope instabilities increased
517 drastically after major service road constructions for hydroelectric power plants and as well as
518 other road extension works. Despite the high precipitation amounts in the region, naturally
519 occurring landslides represent a minor percentage both in number and landslide-size-
520 characteristics when compared to the equivalent human-induced mass movements. Regardless of
521 the natural hillslope processes at play, the poor implementation of engineering practices able to
522 ensure stable slope conditions in co- and post- construction phases not only resulted in dangerous
523 widespread landslides but also caused a substantial change in the sediment transport along with
524 the river network. We could not access enough information on the potential effects of this to
525 quantify increases in sediment loads. However, in the long term, the coarse nature of the material
526 removed from the slopes could also clog narrow river passages, potentially damming small
527 sections of the river network. This could further induce a chain of disastrous events, which could
528 affect not only people living nearby but also the rich biodiversity of the region that needs to be
529 protected. This actually means that all endemic-rare plant and animal species exist in Kamilet
530 Valley are in danger now because of the poor engineering practice. Our results emphasize the
531 need to consider erosion and post changes in hillslope processes and sediment flux that further
532 lead to additional threats to the local community and biodiversity in response to poor engineering
533 practices any other anthropogenic disturbances.

534 We also stress that the impact of road construction can disturb the natural slope equilibrium to an
535 extent comparable with moderate (larger than 6 M_w) earthquakes. Such an observation implies
536 that human activities can have a large, if not even dominant, impact on landscape evolution and
537 the natural regime of surface processes. This is part of the definition of Anthropocene, an age
538 where our society shapes nature for our purposes, frequently at the risk of damaging ourselves.

539 **Acknowledgments**

540 We are very grateful to Hasan Sıtkı Özkazanç, an environmental activist from Arhavi Doğa
 541 Koruma Platformu, for providing us valuable information regarding the road constructions and
 542 their consequences in the site. Co-seismic landslide inventories we examined are available from
 543 Schmitt et al. (2017) (<https://www.sciencebase.gov/catalog/item/583f4114e4b04fc80e3c4a1a>).
 544 The inventories we mapped for this study are shared through NASA Landslide Viewer
 545 (<https://landslides.nasa.gov>).

546 **References**

- 547 Akbulut, S., & Kurdoglu, O. (2015). Türkiye’de acil ve öncelikle korunmasi gereken bir alan:
 548 Kamilet ve Durguna Vadileri (Arhavi) ve koruma gerekçeleri. *Kastamonu Üniversitesi*
 549 *Orman Fakültesi Dergisi*, 15(2), 279-296 (in Turkish).
- 550 Alan, I., Balci, V., Keskin, H., Altun, I., Boke, N., Demirbag, H., ... Hanilci, N. (2019).
 551 Tectonostratigraphic characteristics of the area between Çayeli (Rize) and Ispir (Erzurum).
 552 *Maden Tetkik ve Arama Dergisi*, 158(158), 1–29.
- 553 Atta-ur-Rahman, Khan, A. N., Collins, A. E., & Qazi, F. (2011). Causes and extent of
 554 environmental impacts of landslide hazard in the Himalayan region: a case study of Murree,
 555 Pakistan. *Natural Hazards*, 57(2), 413–434. <https://doi.org/10.1007/s11069-010-9621-7>
- 556 Barnard, P. L., Owen, L. A., Sharma, M. C., & Finkel, R. C. (2001). Natural and human-induced
 557 landsliding in the Garhwal Himalaya of northern India. *Geomorphology*, 40(1), 21–35.
 558 [https://doi.org/https://doi.org/10.1016/S0169-555X\(01\)00035-6](https://doi.org/https://doi.org/10.1016/S0169-555X(01)00035-6)
- 559 Brown, A. G., Tooth, S., Bullard, J. E., Thomas, D. S. G., Chiverrell, R. C., Plater, A. J., ...
 560 Aalto, R. (2017). The geomorphology of the Anthropocene: emergence, status and
 561 implications. *Earth Surface Processes and Landforms*, 42(1), 71–90.
 562 <https://doi.org/10.1002/esp.3943>
- 563 Brown, A. G., Tooth, S., Chiverrell, R. C., Rose, J., Thomas, D. S. G., Wainwright, J., ...
 564 Downs, P. (2013). The Anthropocene: is there a geomorphological case? *Earth Surface*
 565 *Processes and Landforms*, 38(4), 431–434. <https://doi.org/10.1002/esp.3368>
- 566 Chang, J., & Slaymaker, O. (2002). Frequency and spatial distribution of landslides in a
 567 mountainous drainage basin: Western Foothills, Taiwan. *CATENA*, 46(4), 285–307.

- 568 [https://doi.org/https://doi.org/10.1016/S0341-8162\(01\)00157-6](https://doi.org/https://doi.org/10.1016/S0341-8162(01)00157-6)
- 569 Chen, Y.-J., & Chang, K.-C. (2011). A spatial–temporal analysis of impacts from human
570 development on the Shih-men Reservoir watershed, Taiwan. *International Journal of*
571 *Remote Sensing*, 32(24), 9473–9496. <https://doi.org/10.1080/01431161.2011.562253>
- 572 Clauset, A., Shalizi, C. R., & Newman, M. E. J. (2009). Power-law distributions in empirical
573 data. *SIAM Review*, 51(4), 661–703. <https://doi.org/10.1137/070710111>
- 574 Coker, R. J., & Fahey, B. D. (1993). Road-related mass movement in weathered granite, Golden
575 Downs and Motueka Forests, New Zealand: a note. *Journal of Hydrology (New Zealand)*,
576 31(1), 65–69. Retrieved from <http://www.jstor.org/stable/43944699>
- 577 Dadson, S. J., Hovius, N., Chen, H., Dade, W. B., Lin, J.-C., Hsu, M.-L., ... Stark, C. P. (2004).
578 Earthquake-triggered increase in sediment delivery from an active mountain belt. *Geology*,
579 32(8), 733–736. <https://doi.org/10.1130/G20639.1>
- 580 DOKAP. (2014). *Doğu Karadeniz Projesi (DOKAP) Eylem Planı (2014-2018)*.
- 581 Ersoy, S. (2017). *2016 Yılı Doğa Kaynaklı Afetler Yıllığı “Dünya ve Türkiye.”* Jeoloji
582 Mühendisleri Odası Yayınları No: 129, Ankara (in Turkish).
- 583 Fan, X., Domènech, G., Scaringi, G., Huang, R., Xu, Q., Hales, T. C., ... Francis, O. (2018).
584 Spatio-temporal evolution of mass wasting after the 2008 Mw 7.9 Wenchuan earthquake
585 revealed by a detailed multi-temporal inventory. *Landslides*, 15(12), 2325–2341.
586 <https://doi.org/10.1007/s10346-018-1054-5>
- 587 Fransen, P. J. B., Phillips, C. J., & Fahey, B. D. (2001). Forest road erosion in New Zealand:
588 overview. *Earth Surface Processes and Landforms*, 26(2), 165–174.
589 [https://doi.org/10.1002/1096-9837\(200102\)26:2<165::AID-ESP170>3.0.CO;2-#](https://doi.org/10.1002/1096-9837(200102)26:2<165::AID-ESP170>3.0.CO;2-#)
- 590 Froude, M. J., & Petley, D. N. (2018). Global fatal landslide occurrence from 2004 to 2016.
591 *Natural Hazards and Earth System Sciences*, 18(8), 2161–2181.
592 <https://doi.org/10.5194/nhess-18-2161-2018>
- 593 Guzzetti, F., Malamud, B. D., Turcotte, D. L., & Reichenbach, P. (2002). Power-law correlations
594 of landslide areas in central Italy. *Earth and Planetary Science Letters*, 195(3–4), 169–183.

- 595 [https://doi.org/10.1016/S0012-821X\(01\)00589-1](https://doi.org/10.1016/S0012-821X(01)00589-1)
- 596 Haigh, M. J., Rawat, J. S., & Bartarya, S. K. (1989). Environmental Indicators of Landslide
597 Activity along the Kilbury Road, Nainital, Kumaun Lesser Himalaya. *Mountain Research
598 and Development*, 9(1), 25–33. <https://doi.org/10.2307/3673462>
- 599 Hearn, G. J., & Shakya, N. M. (2017). Engineering challenges for sustainable road access in the
600 Himalayas. *Quarterly Journal of Engineering Geology and Hydrogeology*, 50(1), 69–80.
601 <https://doi.org/10.1144/qjegh2016-109>
- 602 Holcombe, E. A., Beesley, M. E. W., Vardanega, P. J., & Sorbie, R. (2016). Urbanisation and
603 landslides: hazard drivers and better practices. *Proceedings of the Institution of Civil
604 Engineers - Civil Engineering*, 169(3), 137–144. <https://doi.org/10.1680/jcien.15.00044>
- 605 Huffman, G., Stocker, E. F., T, B. D., Nelkin, E. J., & Tan, J. (2019). GPM IMERG Final
606 Precipitation L3 1 day 0.1 degree x 0.1 degree V06. *Edited by Andrey Savtchenko,
607 Greenbelt, MD, Goddard Earth Sciences Data and Information Services Center (GES
608 DISC).*
- 609 Jaboyedoff, M., Michoud, C., Derron, M. H., Voumard, J., Leibundgut, G., Sudmeier-Rieux, K.,
610 ... Leroi, E. (2018). Human-induced landslides: Toward the analysis of anthropogenic
611 changes of the slope environment. *Landslides and Engineered Slopes. Experience, Theory
612 and Practice; CRC Press: Boca Raton, FL, USA*, 217–232.
- 613 Jones, J., Boulton, S., Bennett, G., Whitworth, M., & Stokes, M. (2020). Himalaya mass-
614 wasting: impacts of the monsoon, extreme tectonic and climatic forcing, and road
615 construction. *EGU General Assembly 2020*.
616 <https://doi.org/https://doi.org/10.5194/egusphere-egu2020-8702>
- 617 Khan, S. F., Kamp, U., & Owen, L. A. (2013). Documenting five years of landsliding after the
618 2005 Kashmir earthquake, using repeat photography. *Geomorphology*, 197, 45–55.
619 <https://doi.org/10.1016/j.geomorph.2013.04.033>
- 620 Khattak, G. A., Owen, L. A., Kamp, U., & Harp, E. L. (2010). Evolution of earthquake-triggered
621 landslides in the Kashmir Himalaya, northern Pakistan. *Geomorphology*, 115(1–2), 102–
622 108. <https://doi.org/10.1016/j.geomorph.2009.09.035>

- 623 Larsen, M. C., & Parks, J. E. (1997). How wide is a road? The association of roads and mass-
 624 wasting in a forested montane environment. *Earth Surface Processes and Landforms: The*
 625 *Journal of the British Geomorphological Group*, 22(9), 835–848.
- 626 Lewis, S. L., & Maslin, M. A. (2015). Defining the Anthropocene. *Nature*, 519, 171+.
- 627 Malamud, B. D., Turcotte, D. L., Guzzetti, F., & Reichenbach, P. (2004). Landslide inventories
 628 and their statistical properties. *Earth Surface Processes and Landforms*, 29(6), 687–711.
 629 <https://doi.org/10.1002/esp.1064>
- 630 McAdoo, B. G., Quak, M., Gnyawali, K. R., Adhikari, B. R., Devkota, S., Rajbhandari, P. L., &
 631 Sudmeier-Rieux, K. (2018). Roads and landslides in Nepal: how development affects
 632 environmental risk. *Natural Hazards and Earth System Sciences*, 18(12), 3203–3210.
 633 <https://doi.org/10.5194/nhess-18-3203-2018>
- 634 Morin, G. P., Lavé, J., France-Lanord, C., Rigaudier, T., Gajurel, A. P., & Sinha, R. (2018).
 635 Annual Sediment Transport Dynamics in the Narayani Basin, Central Nepal: Assessing the
 636 Impacts of Erosion Processes in the Annual Sediment Budget. *Journal of Geophysical*
 637 *Research: Earth Surface*, 123(10), 2341–2376. <https://doi.org/10.1029/2017JF004460>
- 638 MTA. (2002). 1:500 000–scale map of Turkey. *General Directorate of Mineral Research and*
 639 *Exploration (MTA), Ankara, Turkey.*
- 640 NASA JPL. (2013). NASA Shuttle Radar Topography Mission United States 1 Arc Second.
 641 NASA EOSDIS Land Processes DAAC, USGS Earth Resources Observation and Science
 642 (EROS) Center, Sioux Falls, South Dakota <https://lpdaac.usgs.gov>, Accessed date: 1
 643 December 2019. Retrieved from
 644 <https://doi.org/10.5067/MEaSURES/SRTM/SRTMUS1.003>
- 645 Nefeslioglu, H. A., Gokceoglu, C., Sonmez, H., & Gorum, T. (2011). Medium-scale hazard
 646 mapping for shallow landslide initiation: the Buyukkoy catchment area (Cayeli, Rize,
 647 Turkey). *Landslides*, 8(4), 459–483. <https://doi.org/10.1007/s10346-011-0267-7>
- 648 Owen, L. A., Kamp, U., Khattak, G. A., Harp, E. L., Keefer, D. K., & Bauer, M. A. (2008).
 649 Landslides triggered by the 8 October 2005 Kashmir earthquake. *Geomorphology*, 94(1–2),
 650 1–9. <https://doi.org/10.1016/j.geomorph.2007.04.007>

- 651 Parker, R. N., Hancox, G. T., Petley, D. N., Massey, C. I., Densmore, A. L., & Rosser, N. J.
 652 (2015). Spatial distributions of earthquake-induced landslides and hillslope preconditioning
 653 in the northwest South Island, New Zealand. *Earth Surface Dynamics*, 3(4), 501–525.
 654 <https://doi.org/10.5194/esurf-3-501-2015>
- 655 Parker, Robert N., Densmore, A. L., Rosser, N. J., De Michele, M., Li, Y., Huang, R., ... Petley,
 656 D. N. (2011). Mass wasting triggered by the 2008 Wenchuan earthquake is greater than
 657 orogenic growth. *Nature Geoscience*, 4(7), 449–452. <https://doi.org/10.1038/ngeo1154>
- 658 Petley, D. (2012). Global patterns of loss of life from landslides. *Geology*, 40(10), 927–930.
 659 <https://doi.org/10.1130/G33217.1>
- 660 Petley, D. N., Hearn, G. J., Hart, A., Rosser, N. J., Dunning, S. A., Oven, K., & Mitchell, W. A.
 661 (2007). Trends in landslide occurrence in Nepal. *Natural Hazards*, 43(1), 23–44.
 662 <https://doi.org/10.1007/s11069-006-9100-3>
- 663 Planet Team. (2017). Planet Application Program Interface: In Space for Life on Earth. San
 664 Francisco, CA. <https://api.planet.com>.
- 665 Poesen, J. (2018). Soil erosion in the Anthropocene: Research needs. *Earth Surface Processes
 666 and Landforms*, 43(1), 64–84. <https://doi.org/10.1002/esp.4250>
- 667 Raja, N. B., Çiçek, I., Türkoğlu, N., Aydın, O., & Kawasaki, A. (2017). Landslide susceptibility
 668 mapping of the Sera River Basin using logistic regression model. *Natural Hazards*, 85(3),
 669 1323–1346. <https://doi.org/10.1007/s11069-016-2591-7>
- 670 Reis, S., Nişancı, R., & Yomralioğlu, T. (2009). Designing and Developing a Province-Based
 671 Spatial Database for the Analysis of Potential Environmental Issues in Trabzon, Turkey.
 672 *Environmental Engineering Science*, 26(1), 123–130. <https://doi.org/10.1089/ees.2007.0158>
- 673 Schmitt, R. G., Tanyas, H., Nowicki Jessee, M. A., Zhu, J., Biegel, K. M., Allstadt, K. E., ...
 674 Knudsen, K. L. (2017). An open repository of earthquake-triggered ground-failure
 675 inventories. In *Data Series*. <https://doi.org/10.3133/ds1064>
- 676 Şekercioğlu, Ç. H., Anderson, S., Akçay, E., & Bilgin, R. (2011). Turkey's rich natural heritage
 677 under assault. *Science*, 334(6063), 1637–1639.

- 678 Şekercioglu, Ç. H., Anderson, S., Akçay, E., Bilgin, R., Can, Ö. E., Semiz, G., ... Nüzhet Dalfes,
 679 H. (2011). Turkey's globally important biodiversity in crisis. *Biological Conservation*,
 680 *144*(12), 2752–2769. [https://doi.org/https://doi.org/10.1016/j.biocon.2011.06.025](https://doi.org/10.1016/j.biocon.2011.06.025)
- 681 Stark, C. P., & Guzzetti, F. (2009). Landslide rupture and the probability distribution of
 682 mobilized debris volumes. *Journal of Geophysical Research: Earth Surface*, *114*(2), 1–16.
 683 <https://doi.org/10.1029/2008JF001008>
- 684 Steffen, W., Broadgate, W., Deutsch, L., Gaffney, O., & Ludwig, C. (2015). The trajectory of the
 685 Anthropocene: The Great Acceleration. *The Anthropocene Review*, *2*(1), 81–98.
 686 <https://doi.org/10.1177/2053019614564785>
- 687 Steffen, W., Grinevald, J., Crutzen, P., & McNeill, John. (2011). The Anthropocene: conceptual
 688 and historical perspectives. *Philosophical Transactions of the Royal Society A:*
 689 *Mathematical, Physical and Engineering Sciences*, *369*(1938), 842–867.
 690 <https://doi.org/10.1098/rsta.2010.0327>
- 691 Tang, C., Zhu, J., Qi, X., & Ding, J. (2011). Landslides induced by the Wenchuan earthquake
 692 and the subsequent strong rainfall event: A case study in the Beichuan area of China.
 693 *Engineering Geology*, *122*(1), 22–33.
 694 [https://doi.org/https://doi.org/10.1016/j.enggeo.2011.03.013](https://doi.org/10.1016/j.enggeo.2011.03.013)
- 695 Tanyaş, H., Allstadt, K. E., & van Westen, C. J. (2018). An updated method for estimating
 696 landslide-event magnitude. *Earth Surface Processes and Landforms*, *43*(9).
 697 <https://doi.org/10.1002/esp.4359>
- 698 Tanyaş, H., van Westen, C. J., Allstadt, K. E., Anna Nowicki Jessee, M., Görüm, T., Jibson, R.
 699 W., ... Hovius, N. (2017). Presentation and Analysis of a Worldwide Database of
 700 Earthquake-Induced Landslide Inventories. *Journal of Geophysical Research: Earth*
 701 *Surface*, *122*(10). <https://doi.org/10.1002/2017JF004236>
- 702 Tanyaş, H., van Westen, C. J., Allstadt, K. E., & Jibson, R. W. (2019). Factors controlling
 703 landslide frequency–area distributions. *Earth Surface Processes and Landforms*, *44*(4).
 704 <https://doi.org/10.1002/esp.4543>
- 705 U.S. Geological Survey. (2017). Search Earthquake Catalog. Retrieved March 2, 2020, from

- 706 <https://earthquake.usgs.gov/earthquakes/search/>
- 707 Valdiya, K. S. (2014). Damming rivers in the tectonically resurgent Uttarakhand Himalaya.
 708 *Current Science*, *106*(12), 1658–1668. Retrieved from
 709 <http://www.jstor.org/stable/24102998>
- 710 Van Den Eeckhaut, M., Poesen, J., Govers, G., Verstraeten, G., & Demoulin, A. (2007).
 711 Characteristics of the size distribution of recent and historical landslides in a populated hilly
 712 region. *Earth and Planetary Science Letters*, *256*(3–4), 588–603.
 713 <https://doi.org/10.1016/j.epsl.2007.01.040>
- 714 Vuillez, C., Tonini, M., Sudmeier-Rieux, K., Devkota, S., Derron, M.-H., & Jaboyedoff, M.
 715 (2018). Land use changes, landslides and roads in the Phewa Watershed, Western Nepal
 716 from 1979 to 2016. *Applied Geography*, *94*, 30–40.
 717 <https://doi.org/https://doi.org/10.1016/j.apgeog.2018.03.003>
- 718 Waters, C. N., Zalasiewicz, J., Summerhayes, C., Barnosky, A. D., Poirier, C., Gąsuzka, A., ...
 719 Wolfe, A. P. (2016). The Anthropocene is functionally and stratigraphically distinct from
 720 the Holocene. *Science*, *351*(6269), aad2622. <https://doi.org/10.1126/science.aad2622>
- 721 WWF. (2020). Kamilet Havzası Bir Doğa Müzesi Olarak Saklanmalı. Retrieved from
 722 https://www.wwf.org.tr/yayinlarimiz/basin_bultenleri/?10060/Kamilet-Havzasi-Bir-Doga-
 723 [Muzesi-Olarak-Saklanmali](https://www.wwf.org.tr/yayinlarimiz/basin_bultenleri/?10060/Kamilet-Havzasi-Bir-Doga-Muzesi-Olarak-Saklanmali)
- 724 Xu, C., Xu, X., Shyu, J. B. H., Zheng, W., & Min, W. (2014). Landslides triggered by the 22
 725 July 2013 Minxian-Zhangxian, China, Mw 5.9 earthquake: Inventory compiling and spatial
 726 distribution analysis. *Journal of Asian Earth Sciences*, *92*(July 2013), 125–142.
 727 <https://doi.org/10.1016/j.jseaes.2014.06.014>
- 728 Yuksel, E., & Eminagaoglu, O. (2017). Flora Of The Kamilet Valley (Arhavi, Artvin, Turkey).
 729 *International Journal of Ecosystems and Ecology Science-IJEES*, *7*(4), 905–914.
- 730
- 731
- 732

